



Published in final edited form as:

Nature. 2009 December 24; 462(7276): 1070–1074. doi:10.1038/nature08622.

Novel mutant-selective EGFR kinase inhibitors against EGFR T790M

Wenjun Zhou^{1,2,#}, Dalia Ercan^{3,4,#}, Liang Chen^{3,4,#}, Cai-hong Yun^{1,2,#}, Danan Li^{3,4}, Marzia Capelletti^{3,4}, Alexis B. Cortot^{3,4}, Lucian Chirieac⁵, Roxana E. Iacob^{6,7}, Robert Padera⁵, John R. Engen^{6,7}, Kwok-Kin Wong^{3,4,8,¶}, Michael J. Eck^{1,2,¶}, Nathanael S. Gray^{1,2,¶,**}, and Pasi A. Jänne^{3,4,8,¶}*

¹Department of Cancer Biology, Dana Farber Cancer Institute, Boston, MA

²Department of Biological Chemistry and Molecular Pharmacology, Dana Farber Cancer Institute, Boston, MA

³Lowe Center for Thoracic Oncology, Dana-Farber Cancer Institute, Boston, MA

⁴Department of Medical Oncology, Dana-Farber Cancer Institute, Boston, MA

⁵Department of Pathology, Brigham and Women's Hospital, Boston, MA

⁶The Barnett Institute of Chemical & Biological Analysis, Northeastern University, Boston, MA

⁷Department of Chemistry and Chemical Biology, Northeastern University, Boston, MA

⁸Department of Medicine, Brigham and Women's Hospital and Harvard Medical School, Boston, MA

Abstract

The clinical efficacy of epidermal growth factor receptor (EGFR) kinase inhibitors in *EGFR* mutant non-small cell lung cancer (NSCLC) is limited by the development of drug resistance mutations, including the gatekeeper T790M mutation¹⁻³. Strategies aimed at targeting EGFR T790M with irreversible inhibitors have had limited success and are associated with toxicity due to concurrent inhibition of wild type EGFR^{4,5}. All current EGFR inhibitors possess a structurally related quinazoline based core scaffold and were identified as ATP-competitive inhibitors of wild type EGFR. Here we identify a covalent pyrimidine EGFR inhibitor by screening an irreversible kinase inhibitor library specifically against EGFR T790M. These agents are 30-100 fold more potent against EGFR T790M, and up to 100 fold less potent against wild type EGFR, than quinazoline based EGFR inhibitors *in vitro* and are effective in murine models of lung cancer driven by EGFR T790M. Co-crystallization studies reveal a structural basis for the increased potency and mutant selectivity of these agents. These mutant selective irreversible EGFR kinase inhibitors may be clinically more

* Address Correspondence to either: Pasi A. Jänne, M.D., Ph.D., Lowe Center for Thoracic Oncology, Dana-Farber Cancer Institute, D820, 44 Binney Street, Boston, MA 02115, Phone: (617) 632-6076, Fax: (617) 582-7683, pjanne@partners.org, Nathanael S. Gray, Ph.D., Department of Biological Chemistry and Molecular Pharmacology, 250 Longwood Avenue., Seeley G. Mudd building; 628A, Boston, MA 02115, Phone: (617) 582-8590, Fax: (617) 582-8615, Nathanael_Gray@dfci.harvard.edu.

#These authors contributed equally to this work

¶These laboratories contributed equally to this work

Correspondence and requests for materials should be addressed to either N.S.G. (Nathanael_Gray@dfci.harvard.edu) or P.A.J. (pjanne@partners.org).

Author Contributions W.Z., D.E., L.C., C.Y., D.L., M.C. A.B.C. designed experiments, conducted studies and analyzed data. R.E.I. and J.R.E. performed and analyzed the mass spectrometry studies. L.C. and R.P. performed the histologic and immunohistochemistry analyses. M.J.E., K.-K.W., N.S.G. and P.A.J. designed the experiments, analyzed data and wrote the manuscript.

Author Information Structural data have been deposited in the Protein Data Bank under the accession code 3IKA.

Full Methods and any associated references are located in the Supplementary Methods.

effective and better tolerated than quinazoline based inhibitors. Our findings demonstrate that functional pharmacological screens against clinically important mutant kinases represent a powerful strategy to identify new classes of mutant selective kinase inhibitors.

Keywords

Epidermal growth factor receptor; mutation; drug resistance; kinase inhibitor

EGFR kinase inhibitors, gefitinib and erlotinib, are effective clinical therapies for NSCLCs that harbor activating mutations in the *EGFR* kinase domain^{1,6}. The most common *EGFR* mutations, L858R and delE746_A750, impart both an increased affinity for gefitinib or erlotinib and a decreased affinity for ATP relative to wild type (WT) EGFR^{7,8}. The clinical efficacy of gefitinib/erlotinib is however ultimately limited by the development of acquired drug resistance such as by mutation of the gatekeeper T790 residue (T790M) which is detected in 50% of clinically resistant patients^{2,3}. Unlike the analogous T315I mutation in ABL, which introduces a steric impediment for imatinib binding, EGFR T790M only modestly effects gefitinib binding but more importantly restores the affinity for ATP, similar to that of WT EGFR⁹.

Most EGFR inhibitors are based on a 4-anilinoquinazoline core scaffold and were initially identified as ATP-competitive inhibitors of WT EGFR. This includes irreversible inhibitors that, unlike gefitinib, contain an electrophilic functionality which undergoes a Michael addition reaction with a conserved cysteine residue present in EGFR (Cys797). The covalent nature of these compounds allows them to achieve greater occupancy of the ATP-site relative to reversible inhibitors providing the ability to inhibit EGFR T790M in pre-clinical models, in spite of the increased ATP affinity conferred by this secondary mutation^{4,10,11}. However, all current irreversible inhibitors are less potent in cell line models harboring *EGFR* T790M compared to those with an *EGFR* activating mutation alone (Figure S1) and at clinically achievable concentrations, these agents do not inhibit EGFR T790M *in vitro*¹⁰⁻¹³. Since the ATP affinity of EGFR T790M is similar to WT EGFR, the concentration of quinazoline-based EGFR inhibitors required to inhibit EGFR T790M, will also effectively inhibit WT EGFR. In patients, this concurrent inhibition of WT EGFR, results in skin rash and diarrhea, and limits the ability to achieve plasma concentrations sufficient to inhibit EGFR T790M. As a consequence the clinical efficacy of the irreversible EGFR inhibitors CI-1033, HKI-272 and PF00299804 has been limited, especially in gefitinib/erlotinib resistant NSCLC patients, and the dose limiting toxicity has been diarrhea and skin rash^{5,14,15}.

We hypothesized that the anilinoquinazoline scaffold may not be the most potent or specific for inhibiting EGFR T790M because it relies on the small size and hydrogen bonding interactions with the gatekeeper threonine of WT EGFR. We prepared a focused library of common kinase inhibitor core scaffolds where one of the side chains was modified with an acrylamide group at a position that molecular modeling predicted to react with Cys 797. This library was screened for compounds that could inhibit the growth of both gefitinib resistant (PC9GR; delE746_A750/T790M) and sensitive (PC9; delE746_A750) cell lines but were not toxic up to 10 μ M against A549 (*KRAS* mutant) or H3122 (*EML4-ALK*) cells. We compared our findings to both reversible (gefitinib) and irreversible EGFR inhibitors (CL-387,785 and HKI-272). Three closely related pyrimidines, WZ3146, WZ4002, and WZ8040 were identified from the screen that possessed up to a 300-fold lower IC₅₀ against the PC9GR cells compared to clinical stage inhibitors such as HKI-272 (Figures 1A, 1B and Table S1). We observed a similar increased potency of the WZ compounds in the H1975 (L858R/T790M) cell line and in Ba/F3 cells harboring *EGFR* T790M (Figure 1B and Tables S1 and S2). The increased cellular potency correlated with inhibition of EGFR, AKT and ERK1/2 phosphorylation in

NSCLC cell lines (Figures 1C and S2) and with the more potent inhibition of EGFR phosphorylation by WZ4002 in NIH-3T3 cells expressing different *EGFR* T790M mutant alleles (Figures 1D and S3). The profile against ERBB2 was markedly different; the WZ compounds were less potent than CL-387,785 or HKI-272 (Tables S1 and S2) and did not inhibit ERBB2 phosphorylation in 3T3 cells expressing the ERBB2 gatekeeper (T798I) mutation (data not shown). Analysis of recombinant EGFR T790M kinase incubated with WZ3146 by electrospray mass spectrometry revealed stoichiometric addition of one inhibitor molecule to the protein. Analysis of a pepsin digest of the modified protein by tandem MS identified Cys 797 as the site of modification thus verifying covalent bond formation between WZ3146 and EGFR (Figure S4).

We profiled WZ3146 and WZ4002 against a panel of 400 kinases using the Ambit kinome screening platform (Table S3 and Figure S5). For WZ4002, kinases that exhibited greater than 95% inhibition relative to the DMSO control (Ambit score < 5) at 10 μ M were selected for measurement of their dissociation constants (Table S3). In addition to EGFR, we observed potent inhibition of several of the ten kinases that possess a cysteine at the same position as EGFR including a subset of the TEC-family kinases (Figure S6). Cross-reactivity with BMX has been reported for irreversible quinazoline-derived EGFR inhibitors¹⁶. To confirm whether the observed binding activity translated into cellular inhibition, WZ4002 and WZ3146 were profiled against Ba/F3 cells transformed with TEL fusions of BMX, BLK, JAK2 and JAK3. WZ4002, which possesses an ortho-methoxy group at the C2-aniline substituent, is more selective for EGFR compared to WZ3146 (Table S4).

We next determined whether the increased potency of the WZ compounds against mutant EGFR also applied to WT EGFR. We used EGFR WT HN11 cells¹⁷ and Ba/F3 cells harboring the EGFR vIII mutation which contains a WT kinase domain (Figure 2A and Table S2). These compounds were 3-100-fold less potent, with WZ4002 being least potent, compared to CL-387,785 and HKI-272 at inhibiting the growth of the *EGFR* WT cells. Furthermore, WZ4002 was 100-fold less effective at inhibiting phosphorylation of WT EGFR compared to the quinazoline inhibitors (Figure 2B). Similarly, WZ4002 inhibited EGFR kinase activity of recombinant L858R/T790M protein more potently than of WT EGFR, while the opposite was observed with HKI-272 and gefitinib (Figures S7A and S7B).

In order to better understand the potency and relative selectivity for EGFR T790M over WT EGFR, we determined the crystal structure of WZ4002 in complex with EGFR T790M (Figures 3A, 3B and S8 and Table S5). The compound binds within the ATP-binding cleft of the enzyme, forming the expected covalent bond with Cys797. As expected based upon co-structures of related pyrimidine derived inhibitors with CDK2¹⁸, JNK1¹⁹, and FAK²⁰, the anilinopyrimidine core of WZ4002 forms a bidentate hydrogen bonding interaction with the 'hinge' residue Met 793 (Figure 3B). The chlorine substituent on the pyrimidine ring contacts the mutant gatekeeper residue, Met790. The hydrophobicity conferred by this mutation likely contributes to the potency of these compounds against the T790M mutant. The aniline ring forms a hydrophobic interaction with the α -carbon of Gly796 and its methoxy substituent extends toward Leu792 and Pro794 in the hinge region. The greater selectivity of the WZ4002 compound likely derives from the fact that both JAK3 and TEC-family kinases have a bulkier residue (tyrosine in JAK3, phenylalanine in TEC-family) in the position of Leu792, which would be expected to sterically interfere with the methoxy group in WZ4002. The reactive acrylamide moiety and the linking phenyl ring comprise the other arm of the inhibitor. The "linker" phenyl ring lies roughly perpendicular to the pyrimidine core; this orientation juxtaposes the acrylamide with the thiol of Cys797 for covalent bond formation (Figure 3B).

We further determined whether WZ4002 is effective *in vivo* using mouse lung cancer models harboring either *EGFR* L858R/T790M or Del E746_A750/T790M. We chose WZ4002 for the

in vivo studies because *in vitro* it was least potent against WT EGFR and against other cysteine containing kinases (Tables S2 and S4) but was effective against EGFR T790M. A pharmacokinetic study was performed to determine the achievable plasma concentration (429ng/ml), half life (2.5 hours), and the oral bioavailability (24%) of WZ4002 (Tables S6, S7 and S8). In a pharmacodynamic study WZ4002 effectively inhibited EGFR, AKT and ERK1/2 phosphorylation (Figure 4A) which was associated with a significant increase in TUNEL positive and a significant decrease in Ki67 positive cells compared to vehicle alone treated mice (Figures 4B and 4C). To evaluate whether WZ4002 imparted a differential effect on WT EGFR *in vivo*, we evaluated EGFR phosphorylation in the hair bulb from mouse skin following treatment with either erlotinib or WZ4002 (Figures 2C and 2D). Only erlotinib significantly inhibited EGFR phosphorylation in the hair bulb. In a 2 week efficacy study, WZ4002 treatment resulted in significant tumor regressions compared to vehicle alone in both T790M containing murine models (Figures 4D, 4E and S9). Histological evaluation of the lungs following treatment confirmed significant resolution of the tumor nodules with only few small residual nodules and nodule remnants that had evidence of treatment effect with decreased cellularity and increased fibrosis consistent with remodeling/scarring (Figure 4F). There were no signs of overt toxicity compared with vehicle treated mice during the study as assessed by changes in weight (data not shown), serum creatine and total white blood cell count (Figure S10).

Our studies identify a novel structural class of EGFR kinase inhibitors which are effective *in vitro* and *in vivo* models harboring the *EGFR* T790M mutation. Given the dramatic activity in models with established *EGFR* T790M, we determined whether WZ4002 treatment could also *prevent* the development of *EGFR* T790M using *in vitro* models harboring *EGFR* activating mutations. Unlike with gefitinib or HKI-272, which when used at their achievable plasma concentrations lead to development of *EGFR* T790M *in vitro*^{13,21,22}, we were unable to isolate any *EGFR* T790M containing clones from WZ4002 treated Ba/F3 or PC9 NSCLC cells (Table S9). These findings suggest that WZ4002 could also be used as initial therapy for *EGFR* mutant NSCLC patients and may ultimately lead to a longer time to disease progression than currently achieved with gefitinib¹.

Our crystallographic studies provide insight as to why WZ4002 is so much more effective against L858R/T790M than HKI-272. Although both share the irreversible component, the anilinopyrimidine scaffold of WZ4002 is an intrinsically better fit for the mutant gatekeeper methionine (Figure S11). To further test this hypothesis we prepared WZ4003, a reversible analog of WZ4002 which is non-reactive toward Cys797. WZ4003 binds to the L858R/T790M mutant 100-fold more tightly than it does to the WT EGFR (Table S10), confirming that the scaffold *per se* is indeed specific for the mutant kinase. Importantly, the WZ compounds rely on covalent bond formation for potent cellular inhibition, as evidenced by the 100-fold increase in IC₅₀ of WZ4002 against the *EGFR* C797S mutants and by the significantly reduced cellular IC₅₀ of WZ4003 against T790M containing Ba/F3 cells (Table S2). These observations highlight the importance of using a library of *irreversible* kinase inhibitors, as WZ4003 would not have been identified in the initial cellular screen.

Mutations, including at the gatekeeper residue, are a common mechanism of drug resistance to kinase inhibitors. The current approach, using a cellular screen expressing the mutant kinase of interest, can be applied to identify novel agents specifically against drug resistance or oncogenic mutations implicated in human cancers. Such agents may truly be cancer selective and clinically more potent and less toxic than those that also concurrently inhibit the wild type kinase. The agents described here are unique in that they inhibit both the drug sensitizing and resistance mutations but are selective against WT EGFR^{23,24,25}. Further studies are needed to determine whether this class of EGFR inhibitors will be clinically effective in patients with *EGFR* mutant cancers harboring *EGFR* T790M mediated acquired drug resistance.

Methods Summary

Kinase inhibitors

Gefitinib, CL-387,785 and HKI-272 were obtained from commercial sources. The WZ compounds were synthesized using a four step chemical synthesis and described in detail in the Supplementary Methods. The final products were verified by ¹H nuclear magnetic resonance (NMR) and LCMS.

Cell lines

EGFR wild type and mutant NSCLC, Ba/F3 cells and NIH-3T3 cells were cultured as previously described¹⁰. The PC9GR4 cells were generated as previously described and verified to contain *EGFR* delE746_A750/T790M by direct sequencing²¹. Cell proliferation and growth assays were performed using the MTS assay as previously described²⁶. Site directed mutagenesis was performed using the Quick Change Site-Directed Mutagenesis kit (Stratagene; La Jolla, CA) according to the manufacturer's instructions.

EGFR kinase assays

In vitro inhibitory enzyme kinetic assays using recombinant *EGFR* L858R/T790M and WT protein and were performed using the ATP/NADH coupled assay system in a 96-well format as previously described⁷.

Crystal structure determination and refinement

The structure of WZ4002 in complex with *EGFR* T790M was determined as previously described⁹.

Mouse studies

All studies involving mice were approved by the Dana Farber Cancer Institute Animal Care and Use Committee. *EGFR*-TL (T790M/L858R) mice were generated as previously described⁴. *EGFR* exon19 Deletion-T790M (TD) inducible bitransgenic mice were similarly generated and characterized. Mice were treated either with vehicle (NMP (10% 1-methyl-2-pyrrolidinone: 90% PEG-300) alone or WZ4002 at 25mg/kg gavage daily and followed by MRI scanning as previously described^{4,27}. Histology, immunohistochemistry and immunoblotting analyses were performed according to standard protocols, as previously described^{4,10}.

Generation of drug resistant cells

N-ethyl-N-nitrosourea (ENU) mutagenesis was carried out using *EGFR* L858R and DelE746_A750 Ba/F3 cells as previously described²⁸. Treated cells were expanded in 100 nM WZ4002, 1 μM WZ4002, 200 nM HKI-272 or 1 μM gefitinib and resistant clones isolated and further characterized.

Supplementary Material

Refer to Web version on PubMed Central for supplementary material.

Acknowledgments

This study is supported by grants from the National Institutes of Health RO1CA11446 (P.A.J.), R01CA135257 (P.A.J.), R01CA080942 (M.J.E.), R01CA130876-02 (N.S.G.), R01CA116020 (M.J.E.), R01AG2400401 (K.-K.W.), R01 CA122794 (K.-K.W.), R01GM070590 (J.R.E.), National Cancer Institute Lung SPORE P50CA090578 (P.A.J. and K.-K.W.), the Cecily and Robert Harris Foundation (K.-K.W.), Uniting Against Lung Cancer (K.-K.W.), the Flight Attendant Medical Research Institute (K.-K.W.), the Hazel and Samuel Bellin research fund (P.A.J.) and the Damon

Runyon Foundation Cancer Innovation Award (N.S.G.). This work is contribution 948 from the Barnett Institute. Dr. Janne receives royalties as a co-inventor on a patent awarded for the discovery of *EGFR* mutations, licensed to Genzyme Genetics, which was not involved in this study. M.J.E. is a consultant for and receives research support from Novartis Institutes for Biomedical Research. N.S.G., M.J.E. and P.A.J. are co-inventors on a provisional patent application covering the inhibitors described in the manuscript which has been licensed to Gatekeeper Pharmaceuticals in which N.S.G., K.-K.W. and P.A.J. are co-founders. The authors would like to thank Sai Advantium Pharma Limited for performing the pharmacokinetic studies.

References

1. Mok TS, et al. Gefitinib or carboplatin-paclitaxel in pulmonary adenocarcinoma. *N Engl J Med* 2009;361:947–957. [PubMed: 19692680]
2. Pao W, et al. Acquired Resistance of Lung Adenocarcinomas to Gefitinib or Erlotinib Is Associated with a Second Mutation in the EGFR Kinase Domain. *PLoS Med* 2005;2:1–11.
3. Kobayashi S, et al. EGFR mutation and resistance of non-small-cell lung cancer to gefitinib. *N Engl J Med* 2005;352:786–792. [PubMed: 15728811]
4. Li D, et al. Bronchial and peripheral murine lung carcinomas induced by T790M-L858R mutant EGFR respond to HKI-272 and rapamycin combination therapy. *Cancer Cell* 2007;12:81–93. [PubMed: 17613438]
5. Besse B, et al. Neratinib (HKI-272), an irreversible pan-ErbB receptor tyrosine kinase inhibitor: preliminary results of a phase 2 trial in patients with advanced non-small cell lung cancer. *European Journal of Cancer* 2008;6:64. abstract 203.
6. Rosell R, et al. Screening for epidermal growth factor receptor mutations in lung cancer. *N Engl J Med* 2009;361:958–967. [PubMed: 19692684]
7. Yun CH, et al. Structures of lung cancer-derived EGFR mutants and inhibitor complexes: mechanism of activation and insights into differential inhibitor sensitivity. *Cancer Cell* 2007;11:217–227. [PubMed: 17349580]
8. Carey KD, et al. Kinetic analysis of epidermal growth factor receptor somatic mutant proteins shows increased sensitivity to the epidermal growth factor receptor tyrosine kinase inhibitor, erlotinib. *Cancer Res* 2006;66:8163–8171. [PubMed: 16912195]
9. Yun CH, et al. The T790M mutation in EGFR kinase causes drug resistance by increasing the affinity for ATP. *Proc Natl Acad Sci U S A* 2008;105:2070–2075. [PubMed: 18227510]
10. Engelman JA, et al. PF00299804, an irreversible pan-ERBB inhibitor, is effective in lung cancer models with EGFR and ERBB2 mutations that are resistant to gefitinib. *Cancer Res* 2007;67:11924–11932. [PubMed: 18089823]
11. Li D, et al. BIBW2992, an irreversible EGFR/HER2 inhibitor highly effective in preclinical lung cancer models. *Oncogene*. 2008
12. Yuza Y, et al. Allele-Dependent Variation in the Relative Cellular Potency of Distinct EGFR Inhibitors. *Cancer Biol Ther* 2007;6
13. Godin-Heymann N, et al. The T790M “gatekeeper” mutation in EGFR mediates resistance to low concentrations of an irreversible EGFR inhibitor. *Mol Cancer Ther* 2008;7:874–879. [PubMed: 18413800]
14. Janne PA, et al. Preliminary activity and safety results from a phase I clinical trial of PF-00299804, an irreversible pan-HER inhibitor, in patients (pts) with NSCLC. *Journal of Clinical Oncology* 2008;26(Abtract 8027)
15. Janne PA, et al. Multicenter, randomized, phase II trial of CI-1033, an irreversible pan-ERBB inhibitor, for previously treated advanced non small-cell lung cancer. *J Clin Oncol* 2007;25:3936–3944. [PubMed: 17761977]
16. Hur W, et al. Clinical stage EGFR inhibitors irreversibly alkylate Bmx kinase. *Bioorg Med Chem Lett* 2008;18:5916–5919. [PubMed: 18667312]
17. Yonesaka K, et al. Autocrine production of amphiregulin predicts sensitivity to both gefitinib and cetuximab in EGFR wild-type cancers. *Clin Cancer Res* 2008;14:6963–6973. [PubMed: 18980991]
18. Breault GA, et al. Cyclin-dependent kinase 4 inhibitors as a treatment for cancer. Part 2: identification and optimisation of substituted 2,4-bis anilino pyrimidines. *Bioorg Med Chem Lett* 2003;13:2961–2966. [PubMed: 12941312]

19. Alam M, et al. Synthesis and SAR of aminopyrimidines as novel c-Jun N-terminal kinase (JNK) inhibitors. *Bioorg Med Chem Lett* 2007;17:3463–3467. [PubMed: 17459703]
20. Lietha D, Eck MJ. Crystal structures of the FAK kinase in complex with TAE226 and related bis-anilino pyrimidine inhibitors reveal a helical DFG conformation. *PLoS ONE* 2008;3:e3800. [PubMed: 19030106]
21. Ogino A, et al. Emergence of epidermal growth factor receptor T790M mutation during chronic exposure to gefitinib in a non small cell lung cancer cell line. *Cancer Res* 2007;67:7807–7814. [PubMed: 17699786]
22. Engelman JA, et al. Allelic dilution obscures detection of a biologically significant resistance mutation in EGFR-amplified lung cancer. *J Clin Invest* 2006;116:2695–2706. [PubMed: 16906227]
23. Tsai J, et al. Discovery of a selective inhibitor of oncogenic B-Raf kinase with potent antimelanoma activity. *Proc Natl Acad Sci U S A* 2008;105:3041–3046. [PubMed: 18287029]
24. O'Hare T, et al. SGX393 inhibits the CML mutant Bcr-AblT315I and preempts in vitro resistance when combined with nilotinib or dasatinib. *Proc Natl Acad Sci U S A* 2008;105:5507–5512. [PubMed: 18367669]
25. Gontarewicz A, et al. PHA-680626 exhibits anti-proliferative and pro-apoptotic activity on Imatinib-resistant chronic myeloid leukemia cell lines and primary CD34+ cells by inhibition of both Bcr-Abl tyrosine kinase and Aurora kinases. *Leuk Res* 2008;32:1857–1865. [PubMed: 18514829]
26. Engelman JA, et al. MET amplification leads to gefitinib resistance in lung cancer by activating ERBB3 signaling. *Science* 2007;316:1039–1043. [PubMed: 17463250]
27. Ji H, et al. The impact of human EGFR kinase domain mutations on lung tumorigenesis and in vivo sensitivity to EGFR-targeted therapies. *Cancer Cell* 2006;9:485–495. [PubMed: 16730237]
28. Bradeen HA, et al. Comparison of imatinib mesylate, dasatinib (BMS-354825), and nilotinib (AMN107) in an N-ethyl-N-nitrosourea (ENU)-based mutagenesis screen: high efficacy of drug combinations. *Blood* 2006;108:2332–2338. [PubMed: 16772610]

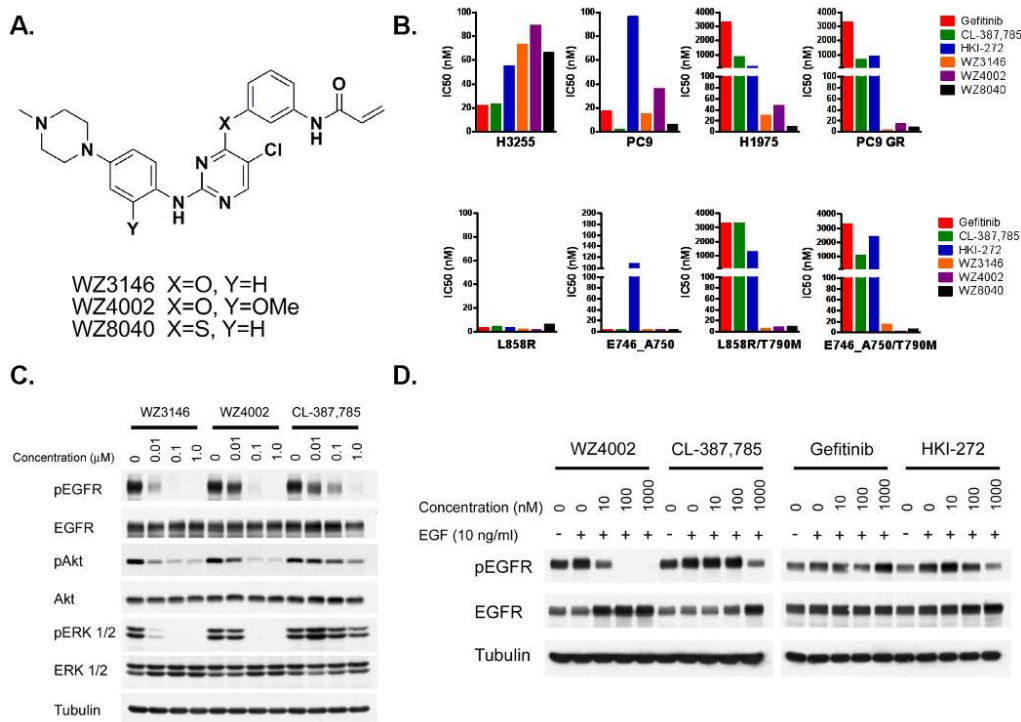


Figure 1. WZ4002, WZ3146 and WZ8040 are novel EGFR inhibitors, suppress the growth of EGFR T790M containing cell lines and inhibit EGFR phosphorylation
A. Chemical structures of the WZ compounds. **B.** IC₅₀ values (nM) for NSCLC cell lines (top) and Ba/F3 (bottom) cells, with genotypes corresponding to the NSCLC cell lines, treated with indicated drugs. Growth was assessed using the MTS survival assay. **C.** Comparison of WZ3146, WZ4002 and CL-387,785 on EGFR signaling in PC9 GR cells. The cells were treated with the indicated concentrations of each drug for 16 hours. Cell extracts were immunoblotted to detect the indicated proteins. **D.** Comparison of EGFR inhibitors on EGFR phosphorylation in 3T3 cells expressing del E746_A750/T90M. The cells were treated with indicated concentrations of each drug for 16 hours and stimulated with EGF (10 ng/ml) 15 minutes prior to lysis. Cell extracts were immunoblotted to detect the indicated proteins.

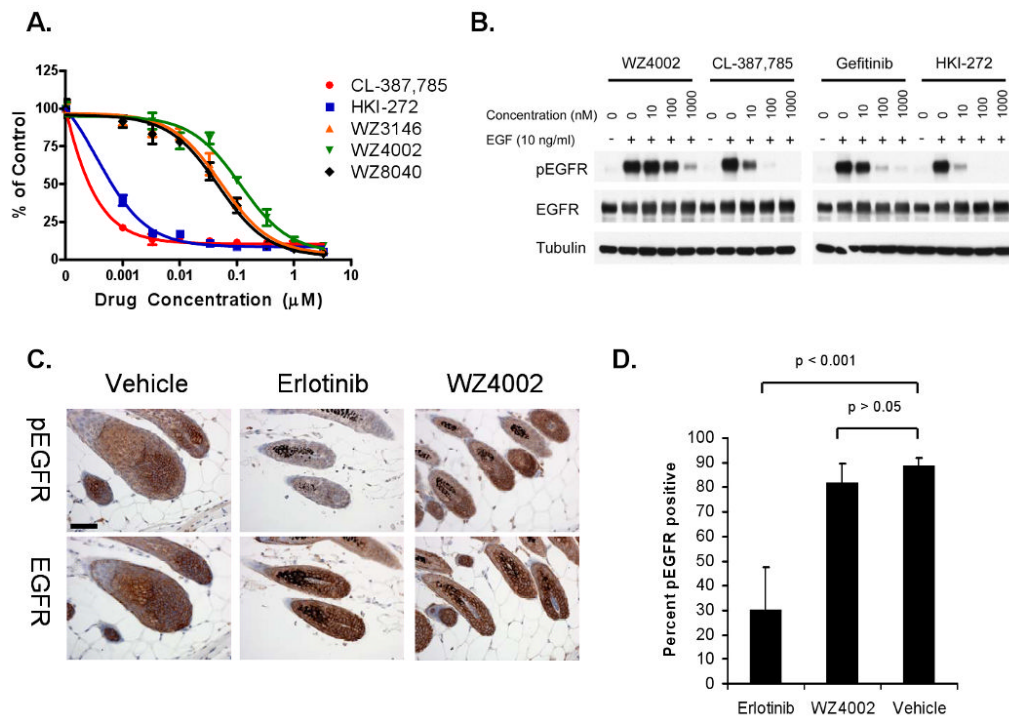


Figure 2. WZ4002 is less potent than quinazoline EGFR inhibitors against wild type EGFR *in vitro* and *in vivo*

A. EGFR vIII Ba/F3 cells treated with WZ or quinazoline EGFR inhibitors. The mean ($n=6$) and standard deviation is plotted for each drug and concentration. **B.** Comparison of EGFR inhibitors on EGFR phosphorylation in 3T3 cells expressing wild type EGFR. The cells were treated with indicated concentrations of each drug for 16 hours and stimulated with EGF (10 ng/ml) 15 minutes prior to lysis. Cell extracts were immunoblotted to detect the indicated proteins. **C.** Immunohistochemical analysis of skin from erlotinib or WZ4002 treated mice using EGFR and pY1173 EGFR. Only erlotinib treatment results in significant inhibition of EGFR phosphorylation. Scale bar, 50 μm . **D.** Quantification of frequency of phospho-EGFR staining from vehicle ($n=3$), erlotinib ($n=3$) and WZ4002 ($n=2$) treated mice. The mean and standard deviations are plotted for drug treatment.

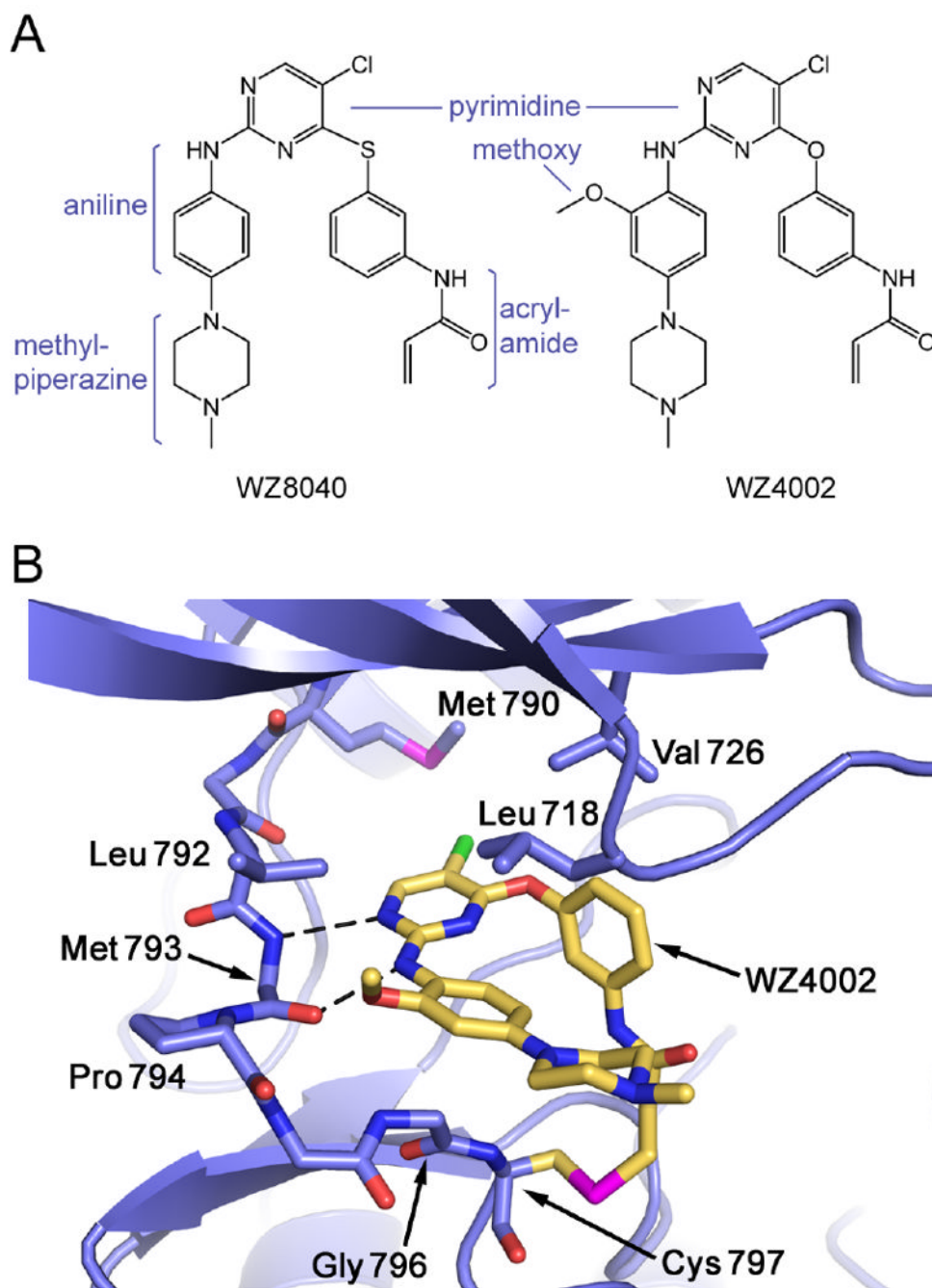


Figure 3. Crystal Structure of WZ4002 bound to EGFR T790M

A. Chemical structures of WZ8040 and WZ4002 are shown schematically in a manner resembling the conformation adopted in complex with the kinase. **B.** Crystal structure of WZ4002 in complex with EGFR T790M mutant (PDB ID 3IKA). WZ4002 binds the active conformation of the kinase, with the both the regulatory C-helix and “DFG” segment of the activation loop in their inward, active positions. The EGFR kinase is shown in a ribbon representation (blue) with the bound inhibitor in yellow. Sidechain and mainchain atoms are shown for selected residues that contact the compound. Expected hydrogen bonds to the backbone amide and carbonyl atoms of Met 793 are indicated by dashed lines. Note also the covalent bond with Cys797. The structure was refined to a crystallographic R value of 21.3%

($R_{\text{free}}=25.4\%$) with data extending to 2.9Å resolution (see methods for further crystallographic details).

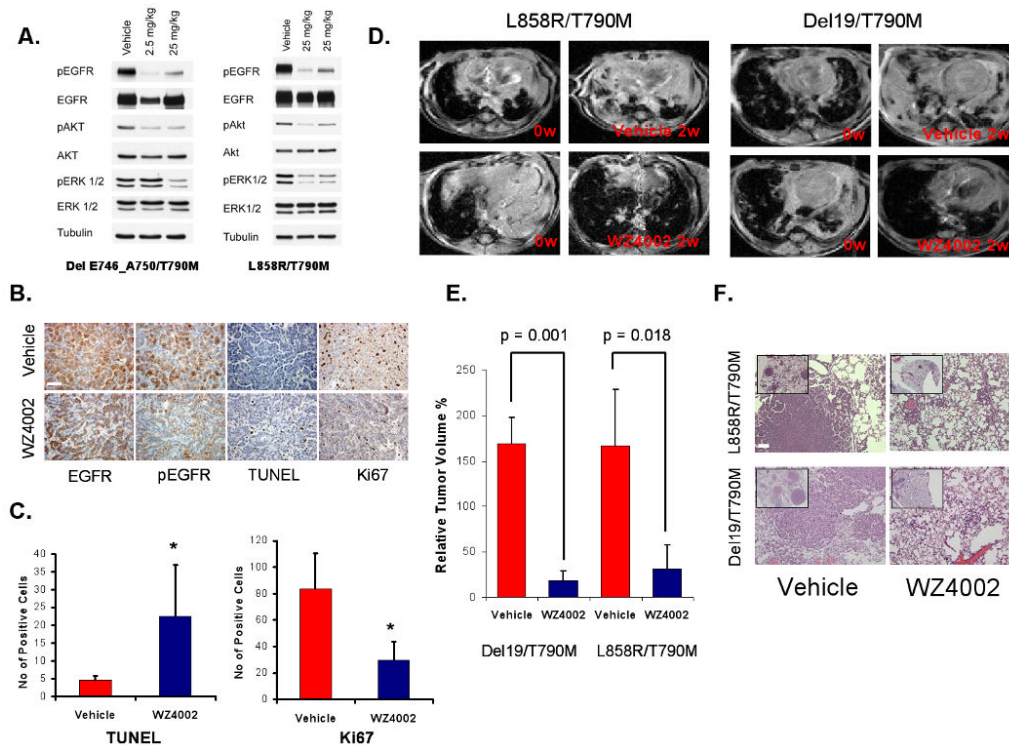


Figure 4. WZ4002 inhibits EGFR phosphorylation and induces significant tumor regression in murine models of EGFR T790M

A. Two doses separated by 16 hours of WZ4002 (2.5 mg/kg or 25 mg/kg) or vehicle were administered to EGFR delE746_A750/T790M or L858R/T790M mice with MRI confirmed tumors. The mice were sacrificed, the lungs isolated and grossly dissected and subjected to cell lysis. Cell extracts were immunoblotted to detect the indicated proteins. **B.** Immunohistochemical analyses of tumors from EGFR delE746_A750/T790M mice from A. using indicated antibodies. Scale bar, 50 μ m. **C.** Quantification of TUNEL and Ki67 positive cells from tumor nodules (n=4) from vehicle and WZ4002 treated mice. The mean and standard deviation are plotted. **D.** MRI images of vehicle or WZ4002 treated mice at baseline (0w) and following 2 weeks (2w) of treatment. **E.** Quantification of the relative tumor volume from MRI images from vehicle treated mice (E746_A750/T790M (n=3); L858R/T790M (n = 4)), and WZ4002 treated L858R/T790M (n=3) and E746_A750/T790M (n=3) mice. The mean and standard deviation are plotted. **F.** Tumors from vehicle and WZ4002 treated mice stained with hematoxylin and eosin. Low power view (inset) demonstrates near complete resolution of tumors in the WZ4002 treated mice. Scale bar, 100 μ m.